Understanding Non-Resolved Space Object Signatures for Space Domain Awareness

Miguel Velez-Reyes[1], Hector Erives[1], Aryzbe Najera[1], Francis Chun[2], Elena Plis[3], Gregory Badura[3], Jacqueline Reyes[1], Michael Gartley[4], Douglas Hope[3], C1C Ethan M. Albrecht[2], Kody A. Wilson [2], David M. Strong[5]

[1]*The University of Texas at El Paso, El Paso, TX 79902*
[2]*U.S. Air Force Academy, Colorado Springs, Colorado 80840*
[3]*Georgia Tech Research Institute, Atlanta, GA, 30318*
[4]*Rochester Institute of Technology, Rochester, NY,*
[5]*Strong EO Imaging, Inc., Colorado Springs, CO 80908*

ABSTRACT

Modeling and understanding signatures and developing the corresponding signature analytics can lead to knowledge generation about non-resolved space objects (NRSO) that can be translated into information exploitation algorithms to infer, classify, predict and diagnose the health of an NRSO for improved space domain awareness (SDA) beyond what is currently possible with light curves. Ground-based observations (new and archived), laboratory measurements, and physics-based simulation models can be used to extract and generate signatures (multi-optical, multi-temporal, and geographically diverse) of measured and modeled behaviors for NRSO. Integrating physics-based models enables controlled experimentation with a broader sense of operational scenarios beyond what may have been captured by ground-based observations. Measured and simulated signatures can be used to build libraries for training of machine learning algorithms or other inference engines as well as mined to translate signatures (or their features) to information.

This paper presents preliminary results of two simulation studies being conducted using the Digital Imaging and Remote Sensing Image Generation (DIRSIG™) to simulate ground-based multi-spectral observations using Johnson-Cousins photometric filters (B, V, R) of resolved and non-resolved space objects. In the first study, we illustrate the integration of laboratory data in a simulation model to study the state of a space asset. Spectral data collected by team members of typical materials used in spacecrafts under pristine and simulated space weather conditions as input to DIRSIG™ to simulate observations of a simple satellite. The changes in the observed simulated ground-based radiance are studied. The purpose is to study the observability of these changes in measured radiance. The second simulation study involves using the DIRSIG™ model to replicate actual ground-based observations of the DirecTV-10 (DTV10, satellite number 31,862) collected between 04:00-08:00 UTC on 23 February 2021 using the US Air Force Academy (USAFA) Falcon Telescope Network (FTN) USAFA-16 telescope. Details on building the simulation model for this satellite are provided. Simulation results show that the simulation model is capable of capturing the shape of the photometric observations which are due to glint produced by the solar panels. However, the resulting simulated model was dimmer than the actual observations.

The results are encouraging but also point to needed additional work before this simulation approach can be utilized as a complement to real observations to understand signatures of NRSO and be used in design, development and validation of algorithms for signature analytics.

1. INTRODUCTION

United States is dependent economically and militarily on space assets [1, 2]. Orbiting satellites provide a multitude of services, which are critical for America's military dominance and economic wealth. Space domain awareness (SDA) is needed to have a clear picture of the environment surrounding US and allied space assets to detect any changes or potential threats. Remote sensing data for SDA is primarily composed of imagery from radar and optical systems [3]. Current ground-based space telescope technology cannot spatially resolve objects in space that are distant (e.g., GEO or XGEO) or that are small (e.g., CubeSats, Parasite Satellites). Furthermore, the low cost of small aperture commercial off-the-shelf (COTS) telescopes is motivating their use for SDA with high spatial diversity even though

they cannot spatially resolve RSO [4, 5, 6, 7]. Radar ground assets are primarily used for observing targets in LEO while optical ground assets are used to assess the environment at higher orbits.

Light curves show the brightness of an non-resolved space object (NRSO) over time observed in a specific viewing geometry. Its temporal variability is due to the superposition of shape, attitude, motion, and material composition of an object under a specific viewing and illumination geometry [8]. Multispectral observations with defined standard sets of passbands, such as Johnson-Cousins photometric filters (B, V, R), provide light curve observations used for multispectral analysis [9], which provides a coarse spectro-temporal signature of the non-resolved space object to be translated by exploitation algorithms into intelligence. Standard astronomical measurements such as photometry, spectroscopy, and polarimetry have been used since the beginning of the space age to characterize a satellite's optical signature [10, 11, 12, 13]. As sensor and computing technology have improved, real-world and simulated data (mostly light curves) allowed researchers to characterize specific satellite attributes such as color classification [14, 15], attitudes and solar panel offsets [16, 17, 18], surface composition and materials [13, 19, 20, 21], shape [18, 22], and the relationship between optical brightness with radar cross section [23].

Remote sensing assets such as hyperspectral and polarization imaging systems are becoming available [24, 25] and the geographical spatial diversity provided by assets such as the US Air Force Academy (USAFA) Falcon Telescope Network (FTN) [7] are bringing enormous amounts of multi-optical data that can provide further insights into aspects of NRSO that were inaccessible with previous remote sensing technologies for SDA. Accurate interpretation of these signatures may allow us to perceive, predict, comprehend, and react appropriately to changing situations in the space environment.

Modeling and understanding signatures and developing the corresponding signature analytics can lead to knowledge generation about NRSO that can be translated into information exploitation algorithms to infer, classify, predict and diagnose the state of a NRSO for improved SDA beyond what is currently possible with light curves. Ground-based observations (new and archived), laboratory measurements, and physics-based simulation models can be used to extract and generate signatures (multi-optical, multi-temporal, and geographically diverse) of measured and modeled behaviors for NRSO. Integrating physics-based models enables controlled computational experimentation with a broader sense of operational scenarios beyond what may have been captured by ground-based observations. Measured and simulated signatures can be used to build spectral libraries that can be used, for instance, for training of machine learning algorithms or other inference engines as well as mined to translate signatures (or their features) to information.

The Digital Imaging and Remote Sensing Image Generation (DIRSIG™) model has been used to model SDA applications. Capabilities of the DIRSIG™ model for SDA applications are described in [26]. This paper presents preliminary results on how a simulation model like this can be used to understand the effects of space weathering on measured radiance and how observed signature of a GEO satellite (DirecTV10) collected with USAFA FTN USAFA-16 telescope at different times correlate with simulated spectro-temporal signatures.

2. DIRSIG™ SIMULATION MODEL

Access to NRSO remote sensing data that provides a rich collection of scenarios is a challenge. Physics-based simulation tools can generate rich data sets complementing observations or laboratory measurements. Rochester Institute of Technology (RIT) has developed and maintains a state-of-the-art image simulation software tool called Digital Imaging and Remote Sensing Image Generation (DIRSIG™), which is a physics-driven synthetic image generation model [27] developed by the RIT Digital Imaging and Remote Sensing Laboratory over the course of 30 years. The model can produce passive multidimensional optical imagery (single-band, multi-spectral, polarimetric, or hyperspectral) from the visible through the thermal infrared region of the electromagnetic spectrum. The tool has the capability to simulate images of a wide variety of resolved and non-resolved space objects across the electromagnetic spectrum, ranging from UV to thermal infrared. DIRSIG™ can incorporate material bidirectional reflectance distribution function (BRDF) and emissivity from laboratory measurements, existing materials databases (such as the AFRL Satellite Assessment Center (SatAC) and Non-Conventional Exploitation Factors (NEF) databases), or based on first-principles for simple materials. Additionally, DIRSIG™ is capable of describing space object motion and articulation from either an externally generated lookup table of values (i.e., generated using Systems ToolKit (STK) [28]) or via a two-line element (TLE) set [29]. Due to the hierarchical nature of the geometry descriptions, the user can specify a time varying articulation of specific space object components such as solar panels that track the sun. With this flexibility, it is straightforward to accurately model the signatures of complex object articulations that

describe things such as rotating solar panels for maximum power transfer, a tumbling rocket body or the deployment of the payload fairing shells during a launch sequence. Capabilities of the DIRSIG for SDA are described in [26, 30].

3. SIMULATING SPACE WEATHERING EFFECTS

Team members from the GTRI and UTEP in collaboration with the SCICL at Kirtland AFRL have collected spectral signatures of typical surface spacecraft materials from polyimide (PI, including different flavors of Kapton©) and polyethylene terephthalate (PET, Mylar© and Melinex©) families, thermal control paints, and solar array coverglasses (CMG, CMX, fused silica) exposed to the different fluences of high-energy (100 keV) electrons mimicking the space environment of GEO orbit. Whereas material degradation in the space environment proceeds as a function of several simultaneous damage mechanisms each driven by a specific type of irradiation, the high-energy electrons is the most damaging species in terms of energy deposition in the GEO environment [31], causing changes in optical, structural, mechanical, charge transport, and chemical properties of spacecraft surface materials [32, 33, 34, 35, 36].

Since each material has a unique spectral fingerprint, changes of its reflectance signature can be used as proxy measurement for other, less convenient measurements. Further, tracking objects in GEO using Earth-based optical observations often consists of the collection of unresolved images of the GEO objects. Brightness of the image is dependent on spacecraft geometry and surface composition. Thus, the composition of the surface and the environment-dependent chemical state of the surface materials may be inferred from the spectral content of an unresolved image, enabling remote diagnosis of spacecraft health.

Directional hemispherical reflectance (DHR) measurements were performed at regular time intervals during the electron irradiation process, for the purpose of dynamic analysis of their optical behavioral changes throughout irradiation. Details of electron irradiation and DHR measurement procedure are reported elsewhere [37, 38]. The DHR spectra of pristine and space-weathered materials can be used as an input to DIRSIG™ software to generate simulated ground-based observations showing the effects of different levels of material weathering at different stages. This simulation experiment will serve to illustrate how laboratory measurements can be integrated with physics-based modeling to understand changes in ground-based observations. This type of analysis can help assess the health of a space asset like DirecTV 10 (DTV-10). Simulation results using DIRSIG™ are presented for the materials shown in Figure 1.

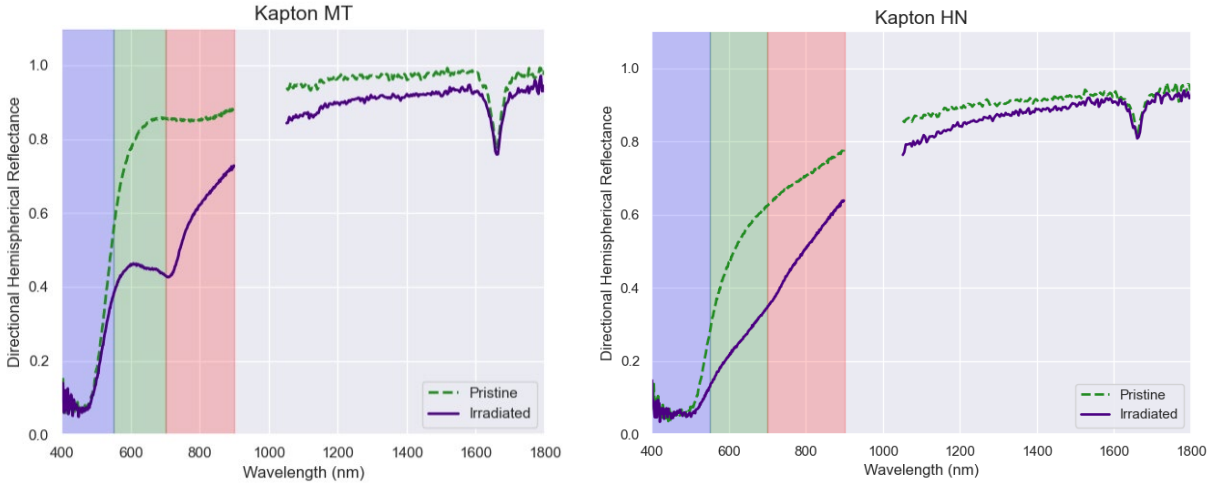

(a) (b)

Figure 1: Pristine and weathered spectra used in simulations: (a) Kapton MT and (b) Kapton HN. Color strips show the location and passband for the Johnson-Cousins photometric filters (B, V, R).

3.1 Simulation Parameters

A simple satellite structure was simulated. The structure consists of solar panel attached to a cube as shown in Figure *2*. The cube is covered with a single material in the simulation. The object is stabilized (not rotating) and an image is collected every 100 seconds. The simulation is run first with the pristine material spectral signature and then with the irradiated signature.

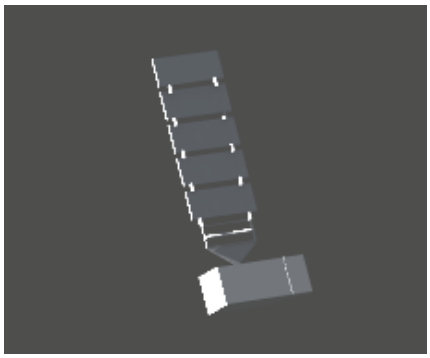

Figure 2: Simple satellite model used for weathering simulations.

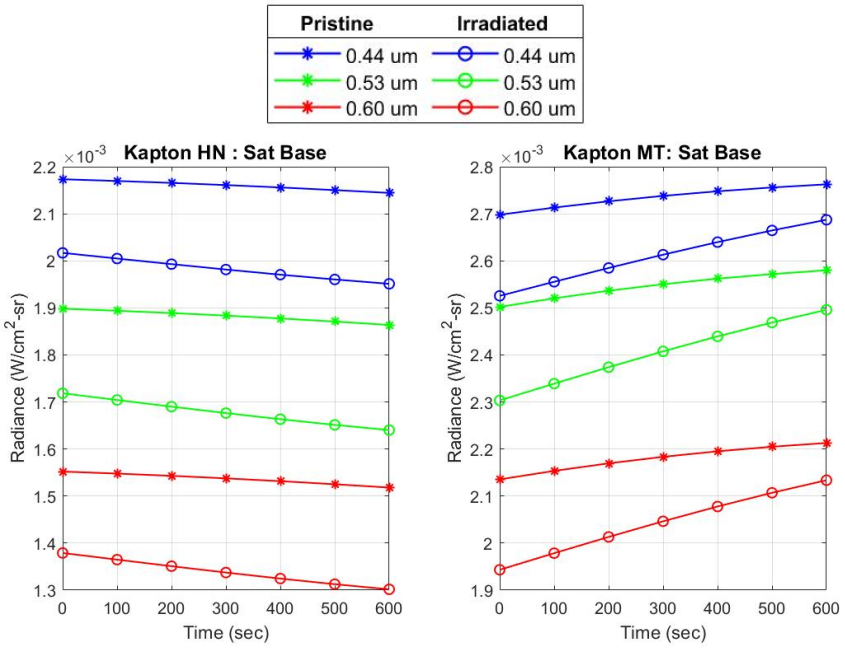

(a) (b)

Figure 3: Simulated ground-based radiance for pristine and irradiated materials: (a) Kapton HN and (b) Kapton MT.

Table 1: Statistics for the difference between the simulated ground-based radiance for pristine and irradiated Kapton HN in $Wm^{-2}sr^{-1}$.

	Mean	RMS	Max	Min
Band 0.44	1.7071E-04	2.2219E-04	4.0700E-04	2.0000E-06
Band 0.53	1.9671E-04	2.5930E-04	4.7800E-04	-4.0000E-06
Band 0.60	1.8986E-04	2.5281E-04	4.6800E-04	-8.0000E-06

Table 2: Statistics for the difference between the simulated ground-based radiance for pristine and irradiated Kapton MT in $Wm^{-2}sr^{-1}$.

	Mean	RMS	Max	Min
Band 0.44	1.2271E-04	3.0053E-04	7.2800E-04	-2.4000E-04
Band 0.53	1.3986E-04	3.5573E-04	8.6100E-04	-2.9200E-04
Band 0.60	1.3400E-04	3.5021E-04	8.4700E-04	-2.9300E-04

Simulated multispectral observations using approximations to the Johnson-Cousins photometric filters (B, V, R) are done and the object is fully resolved. The spectral responses for the three filters are approximated using a Gaussian function with centers at 440 nm (B-filter), 530 nm (V-filter), and 600 nm (R-filter) and a full-width at half max (FWHM) of 50 nm. Ground-based observed radiance is simulated for each case and changes in the measured ground-based radiance due to weathering are evaluated.

3.2 Simulation Results

Simulated results for Kapton HN and Kapton MT are shown in Figure 3. The figures show the ground-based radiance for the Gaussian spectral filters described previously all centered at the center wavelength of the Johnson-Cousins photometric filters (B, V, R). There is a reduction in ground-based radiance from pristine to irradiated as can be expected due to the reduction in reflectance. Statistics on the difference between the simulated ground-based radiance for pristine and irradiated materials are shown in Table 1 and Table 2.

4. MATCHING DIRSIG™ SIMULATION RESULTS TO USAFA-16 OBSERVATIONS

DirecTV-10 (DTV-10, satellite number 31862) is an operational communication GEO satellite, it comprises Kapton© HN, Mylar© M021, and black Kapton© among other surface materials. Ground-based observations of this satellite were collected between 04:00-08:00 UTC on 23 February 2021 using the USAFA-16 telescope. The ground-based optical data includes photometric measurements (Johnson-Cousins B, V, R), slitless spectroscopy (100-lines-per-millimeter transmission grating), and linear polarization signatures (Stokes parameters S0, S1, S2) recently collected over the past couple of years. The simulation results aim at reproducing the collected photometric images. Details of the collection are described in [39].

4.1 Simulation Parameters

To simulate the acquired photometric images, we needed to model the telescope system PSF for each of the Johnson-Cousins photometric filters (B, V, R), and the corresponding filter spectral transmissivity function. As well as a full 3D CAD model for the satellite. This information is input to DIRSIG™ to create the simulated imagery.

The point spread function (PSF) for the USAFA-16 telescope was determined experimentally from photometric images collected with the telescope. To improve SNR on photometric images, five consecutive USAFA-16 images were stacked, and sources are extracted from those images using Photutils, an Astropy package for detection and photometry of astronomical sources [40]. The source radius of aperture set to 1.5 FWHM, inner annulus set to 2.5 FWHM, outer annulus set to $\sqrt{1.5^2 + 2.5^2}$. A 2D Gaussian was fitted to the extracted source to estimate the PSF. The resulting PSF for the R channel is shown in Figure *4*. The parameters for the three fitted Gaussian PSF are given in Table *3*. The spectral transmissivity for the Johnson-Cousins photometric filters (B, V, R) accounting for the Quantum Efficiency (QE) of the camera simulated in DIRSIG™ are shown in Figure 5(a). Spectral reflectance of Si solar panels is shown for reference in Figure *5*. A CAD-model of DTV-10 was provided by the AFRL Satellite Assessment Center (SatAC), along with a comprehensive list of materials, which consists of over 100 materials with reflectance values and Phong and Ward BRDFs. DIRSIG does not support the Phong BRDF, so the Ward BRDF model was used. Pristine spectral signatures were used. Figure 6 shows the CAD model for DTV-10.

Table 3: Parameters for the three fitted 2D Gaussian PSF.

Band	σ_x^2	σ_y^2	θ rotation angle (radians)	Amplitude
R	3.8217	4.5735	-3.9288	1.0026
B	4.5140	5.0683	-0.60198	0.98694
V	4.1513	4.9067	-0.59923	0.96549

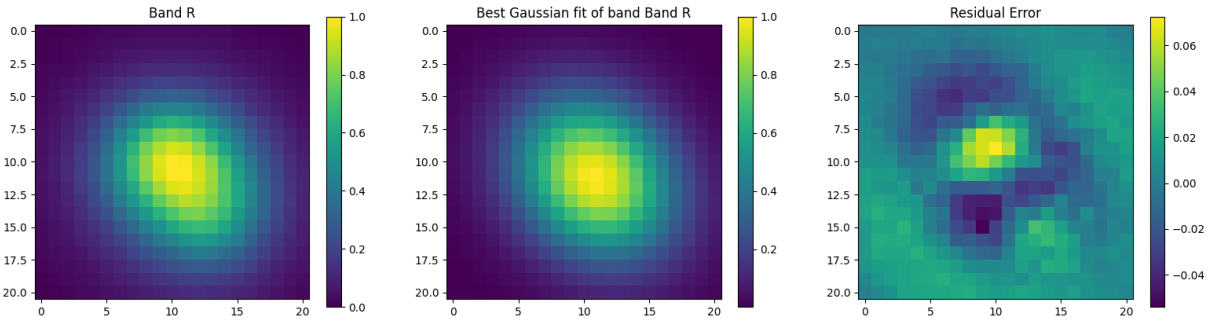

Figure 4: Generated PSFs for the R band.

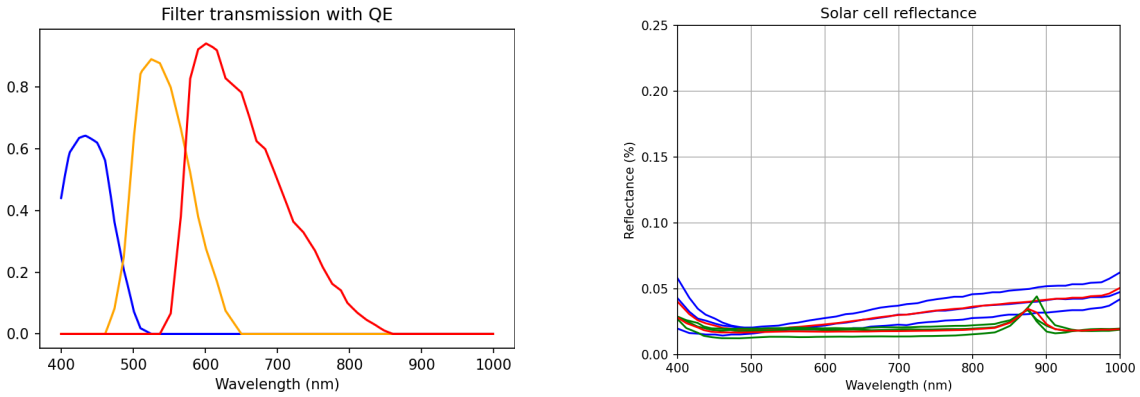

(a) (b)

Figure 5: (a) B V y R filter transmissivity, (b) Si solar cell reflectance values.

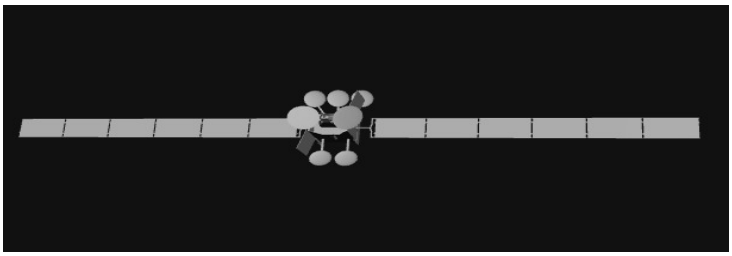

Figure 6: CAD model of DirecTV-10 provided by SatAC.

4.2 Simulation Results

The DIRSIG™ simulations presented here are aimed at reproducing the observations presented in [39]. A mid-latitude winter (MLW) atmospheric model was used in the simulations as it closely matches the atmospheric conditions at the time of the acquisition. The focal length of the simulated telescope is set to be equal to focal length of the USAFA-16 telescope, 3300 mm.

A Python script was written to run the executable file of DIRSIG™ for different satellite poses, i.e., when solar panels are not visible by the camera and when they are, to try to model the same orientation, inclination, and position of the solar panels at that time. The latitude and longitude of the simulated telescope is located at the same coordinates as USAFA-16. The pixel size of the simulated camera matches the pixel size of the actual camera as well, and the size of the simulated images shown here are only 64×64 pixels to reduce simulation time. Two samples of the satellite simulation are shown in Figure 7. Figure 7(a)-(b) show Flux images of the satellite with solar panels configured in such a way that they are not reflecting solar energy towards the sensor. Figure 7(c)-(d) show image of the satellite with solar panels reflecting solar energy towards the sensor.

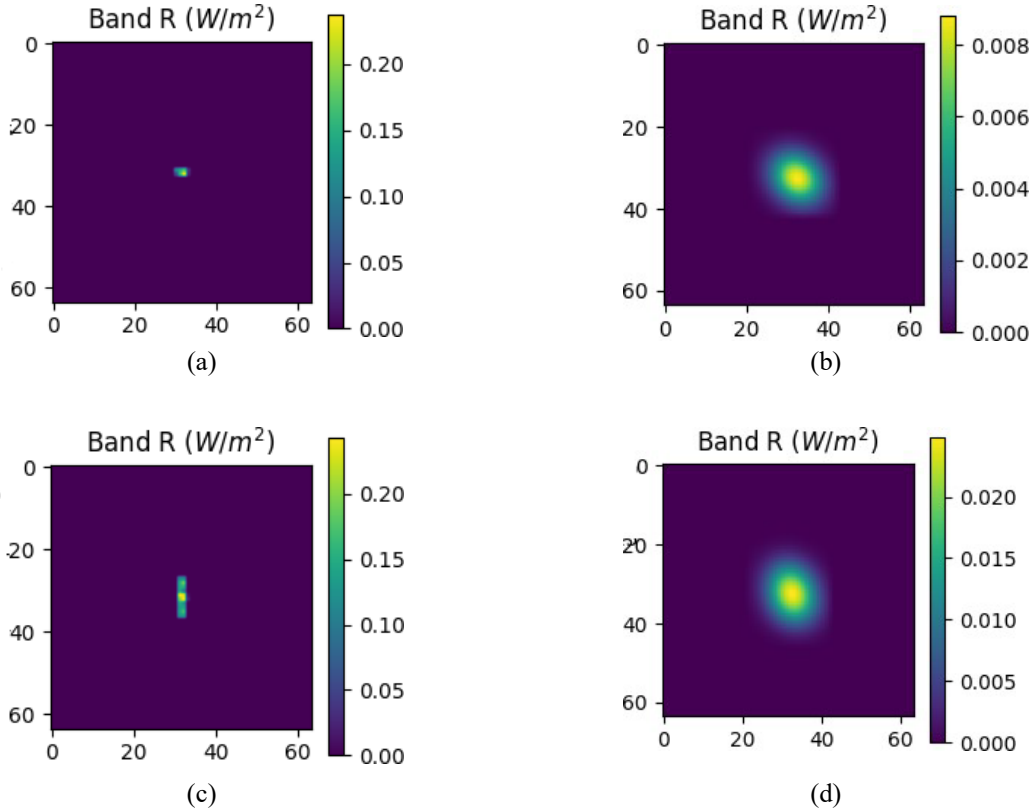

Figure 7: Simulated satellite image without PSF effects (left column) and with PSF effects (right column): (a) and (b) when solar panels are not reflecting solar light in the telescope direction; (c), (d) when solar panels are reflecting light towards the telescope.

The simulated calibrated magnitude value for bands B, V and R for the date of interest are shown in Figure 8. Figure 9 shows the corresponding photometric data measured by USAFA-16 from 04:00-08:00UTC on 23 February 2021. It is notable that the simulation captures the peak in the data related to the satellite glint. This feature was obtained by moving the solar panels, which corroborates what the researchers observed during the glint season in the imagery acquired on February 23, 2021. However, because of the offset in the calibrated magnitude, the simulated calibrated magnitude values seem to be dimmer than those from real measurements. This points to further work in adjusting the simulation parameters to better match the measurement conditions.

5. DISCUSSION AND CONCLUSIONS

Preliminary results presented in this paper show the potential of using a physics-based simulation tool such as DIRSIG™ to generate simulated ground-based observations that could potentially be used to understand signatures of NRSO and use as inputs for the development, testing and validation of information extraction algorithms from remote sensing observations. Clearly challenges remain to properly tune these models to closely reproduce observations and to their eventual use to extrapolate to cases not included in the observational data.

Reflectance changes due to simulated space weathering are reflected in changes in the simulated ground-based observations, thus changes are observable within the simulated conditions. This can be used as input to assess the health of a space asset. The simulations were under conditions where the resident space object was fully resolved. We need to develop further understanding on how observable changes are in the case of an NRSO where the measured spectro-temporal signature is a mixture of all materials in the field of view of the sensor. We also need to test this idea with actual observations of satellites that have been in operation for a long time.

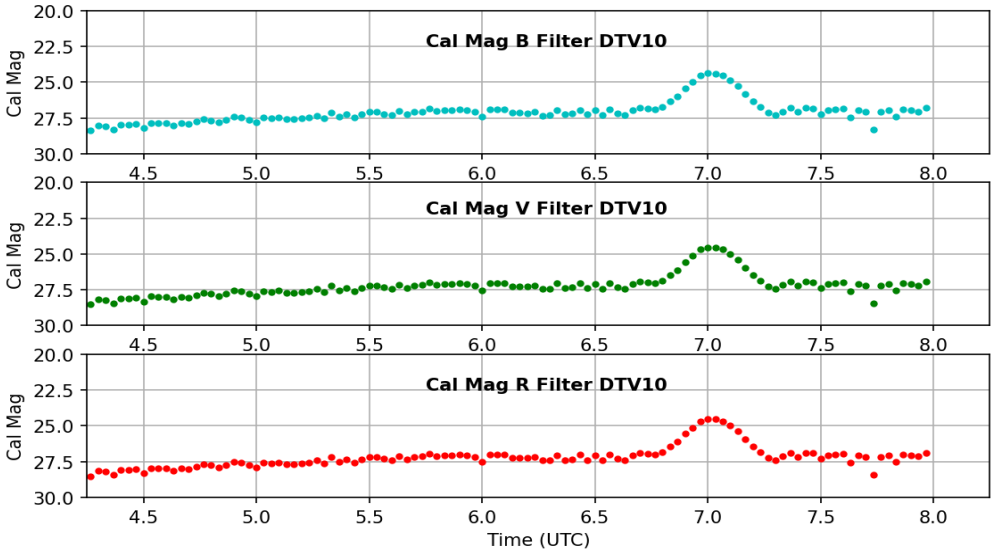

Figure 8: Simulated apparent magnitude values of Johnson-Cousins photometric filters (B, V, R) during the glint season.

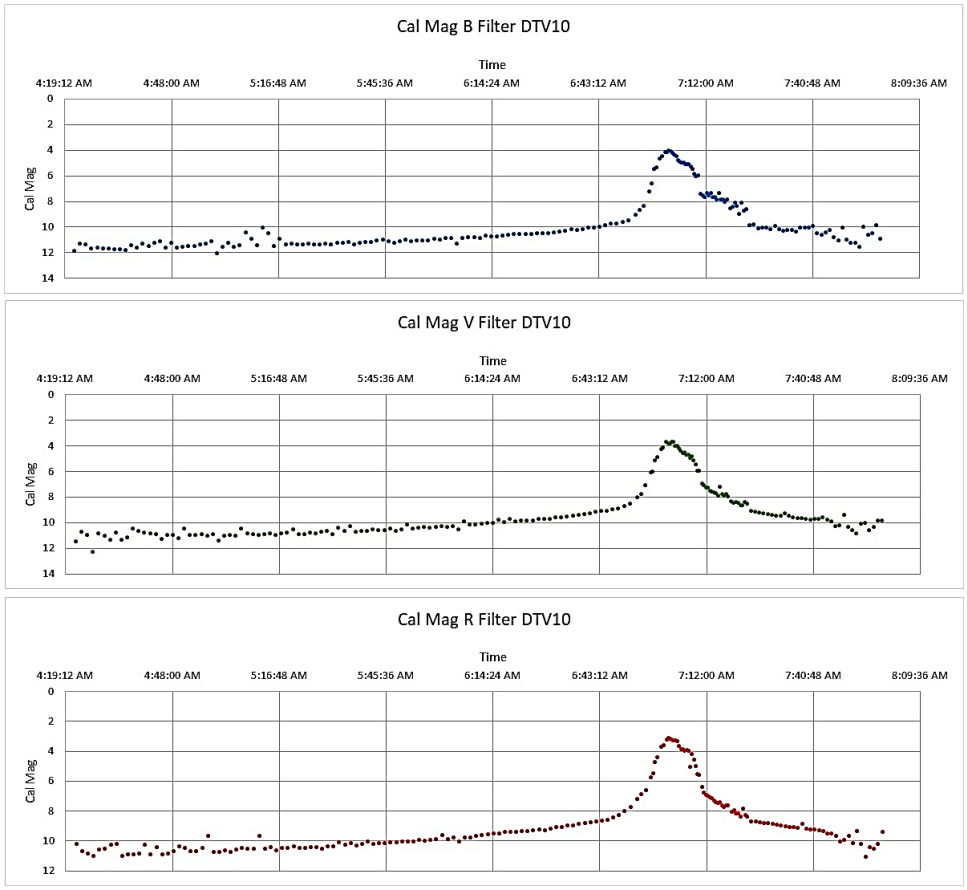

Figure 9: Calibrated magnitude of DTV-10 versus time collected by USAFA-16 using the Johnson-Cousins B filter (blue data points), V filter (green data points) and R filter (red data points).

For the simulation of DTV-10 observations using the USAFA-16 telescope, many improvements are needed to obtain a closer match between the calibrated magnitude values from the simulations and the measurements. In this study only atmospheric conditions, focal length, pixel size, frame size, location of the telescope, TLE of the satellite, filter transmissivity, and quantum efficiency of the camera were adjusted trying to match actual system conditions. Some simulations parameters were found by trial-and-error, which is time consuming and inefficient. Therefore, future work requires further tuning of the simulation parameters and develop approaches for automated tuning the simulation for a broader set of potential cases.

6. ACKNOWLEDGEMENTS

This research made use of the Astropy package for detection and photometry of astronomical sources [40]. Drs. Velez-Reyes, Erives and Najera were partially supported by the Office of the US Assistant Secretary of Defense for Research and Engineering through the Research and Education Program for Historically Black Colleges and Universities and Minority-Serving Institutions (HBCU/MI) under Award No. W911NF-19-1-0011. Dr. Erives would also like to express his gratitude to research engineers Byron Eng and Jeff Bank from RIT for their help and guidance on DIRSIG™, and Lyon G. Luksik form SatAC, who embarked on the efforts to translate an NSM format of the DTV-10 model into the OBJ format. Dr. Erives would also like to thank the AFRL Summer Faculty Fellowship Program for supporting his internship at USAFA during summer 2022. The United States Air Force Academy would like to acknowledge the support of the Air Force Office of Scientific Research. Additionally, this paper is the result of multiple physics senior capstone projects and independent studies at the United States Air Force Academy.

This paper is approved for public release by USAFA: distribution unlimited (USAFA-DF-2022-717).

The views expressed in this article, or presentation are those of the authors and do not necessarily reflect the official policy or position of the United States Air Force Academy, the Air Force, the Department of Defense, or the U.S. Government.

REFERENCES

[1] M. A. Baird, "Maintaining space situational awareness and taking it to the next level," *Air and Space Power Journal,* 2013.

[2] J. W. Crockett, "Space Warfare in the Here and Now: The Rules of Engagement for U.S. Weaponized Satellites in the Current Legal Space Regime," *Journal of Airlaw and Commerce,* vol. 77, 2012.

[3] S. Eves, Space Traffic Control, vol. 251, T. C. Liewen, Ed., American Institute of Aeronautics and Astronautics, Inc., 2017.

[4] N. Estekk, D. Ma and P. Seitzer, "Daylight imaging of LEO satellites using COTS hardware," in *Advanced Maui Optical and Space Surveillance Technologies Conference*, Maui, HI, 2019.

[5] F. Gasdia, A. Barjatya and S. Bilardi, "Multi-Site Simultaneous Time-Resolved Photometry with a Low Cost Electro-Optics System," *Sensors,* vol. 17, p. 1239, May 2017.

[6] J.-H. Park, H.-S. Yim, Y.-J. Choi, J. H. Jo, H.-K. Moon, Y.-S. Park, Y.-H. Bae, S.-Y. Park, D.-G. Roh, S. Cho, E.-J. Choi, M.-J. Kim and J. Choi, "OWL-Net: A global network of robotic telescopes for satellite observation," *Advances in Space Research,* vol. 62, p. 152–163, July 2018.

[7] F. K. Chun, R. D. Tippets, D. M. Strong, D. J. Della-Rose, D. E. Polsgrove, K. C. Gresham, J. A. Reid, C. P. Christy, M. Korbitz, J. Gray and others, "A new global array of optical telescopes: The falcon telescope network," *Publications of the Astronomical Society of the Pacific,* vol. 130, p. 095003, 2018.

[8] C. Fruh and T. Schildknecht, "Analysis of observed and simulated light curves of space debris," in *Proceedings of the international Astronautical Congress*, 2010.

[9] T. E. Payne and S. A. Gregory, "Passive radiometric observations of geosynchronous satellites," in *2004 IEEE Aerospace Conference Proceedings (IEEE Cat. No.04TH8720)*.

[10] R. Tousey, "Optical Problems of the Satellite," *Journal of the Optical Society of America,* vol. 47, p. 261, 4 1957.

[11] K. E. Kissell and R. C. Vanderburgh, "Photoelectric Photometry—A Potential Source for Satellite Signatures," Wright-Patterson AFB, OH, 1966.

[12] R. P. Stead, "An Investigation of Polarization Phenomena Produced by Space Objects," 1967.

[13] J. V. Lambert, "Measurement of the Visible Reflectance Spectra of Orbiting Satellites," Dayton, 1971.

[14] T. E. Payne, S. A. Gregory, N. M. Houtkooper and T. W. Burdullis, "Classification of Geosynchronous Satellites Using Photometric Techniques," in *Advanced Maui Optical and Space Surveillance Technologies Conference*, 2002.

[15] T. E. Payne, S. A. Gregory and J. Villafuerte, "Three-Dimensional Analysis of GEO Photometric Signatures," in *Advanced Maui Optical and Space Surveillance Technologies Conference*, 2004.

[16] T. E. Payne, S. A. Gregory and K. Luu, "SSA Analysis of GEOS Photometric Signature Classifications and Solar Panel Offsets," in *Advanced Maui Optical and Space Surveillance Technologies Conference*, 2006.

[17] D. Hall, J. Africano, D. Archambeault, B. Birge, D. Witte and P. Kervin, "AMOS Observations of NASA's IMAGE Satellite," in *Advanced Maui Optical and Space Surveillance Technologies Conference*, 2006.

[18] D. Hall, B. Calef, K. Knox, M. Bolden and P. Kervin, "Separating Attitude and Shape Effects for Non-resolved Objects," in *Advanced Maui Optical and Space Surveillance Technologies Conference*, 2007.

[19] K. Jorgensen, J. Okada, J. Africano, D. Hall, M. Guyote, K. Hamada, G. Stansbery, E. Barker and P. Kervin, "Reflectance Spectra of Human-Made Space Objects," in *Advanced Maui Optical and Space Surveillance Technologies Conference*, 2004.

[20] K. Abercromby, K. Hamada, M. Guyote, J. Okada and E. S. Barker, "Remote and ground truth spectral measurement comparisons of FORMOSAT III," in *Advanced Maui Optical and Space Surveillance Technologies Conference*, 2007.

[21] D. Hall, K. Hamada, T. Kelecy and P. Kervin, "Surface Material Characterization from Non-resolved Multi-band Optical Observations," in *Advanced Maui Optical and Space Surveillance Technologies Conference*, 2012.

[22] D. O. Fulcoly, K. I. Kalamaroff and F. K. Chun, "Determining Basic Satellite Shape from Photometric Light Curves," *Journal of Spacecraft and Rockets,* vol. 49, p. 76–82, 1 2012.

[23] C. E. Gow, S. Eaves and M. D. Hejduk, "The Visible Magnitude Distribution and Optical Variability of LEO Space Objects," in *Advanced Maui Optical and Space Surveillance Technologies Conference*, 2005.

[24] M. Pirozzoli, L. Zimmerman, M. Korta, A. Scheppe, M. Plummer, F. Chun and D. Strong, "Calibration and sensitivity analysis of a basic polarimeter for manmade satellite observations," in *2020 AMOS Technical Conference Proceedings*, Maui, HI, 2020.

[25] A. Speicher, M. Matin, R. Tippets, F. Chun and D. Strong, "Results from an experiment that collected visible-light polarization data using unresolved imagery for classification of geosynchronous satellites," in *Airborne Intelligence, Surveillance, Reconnaissance (ISR) Systems and Applications XII*, 2015.

[26] Digital Imaging and Remote Sensing Lab, "Space Situational Awareness Handbook," Rochester Institute of Technology, 15 December 2021. [Online]. Available: https://dirsig.cis.rit.edu/docs/new/ssa.html. [Accessed 22 August 2022].

[27] A. A. Goodenough and S. D. Brown, "DIRSIG5: Next-Generation Remote Sensing Data and Image Simulation Framework," *IEEE Journal of Selected Topics in Applied Earth Observations and Remote Sensing,* vol. 10, p. 4818–4833, 11 2017.

[28] Wikipedia, "Systems Tool Kit," 3 2021. [Online]. Available: https://en.wikipedia.org/wiki/Systems_Tool_Kit. [Accessed June 2021].

[29] D. A. Vallado and P. J. Cefola, "Two-line element sets–practice and use," in *63rd International Astronautical Congress*, 2012.

[30] D. Bennett, D. Allen, J. Dank, M. Gartley and D. Tyler, "SSA Modeling and Simulation with DIRSIG," in *Advanced Maui Optical and Space Surveillance Technologies Conference*, 2014.

[31] V. Pilipenko, N. Yagova, N. Romanova and J. Allen, "Statistical relationships between satellite anomalies at geostationary orbit and high-energy particles," *Advances in Space Research,* vol. 37, no. 6, pp. 1192-1205, 2006.

[32] J. Marco and S. Remaury, "Evaluation of Thermal Control Coatings Degradation in Simulated Geo-Space Environment," *High Performance Polymers,* vol. 16, no. 2, pp. 177-196, 2004.

[33] E. A. Plis, D. P. Engelhart, R. Cooper, W. R. Johnston, D. Ferguson and R. Hoffmann, "Review of Radiation-Induced Effects in Polyimide," *Applied Sciences,* vol. 9, no. 10, 2019.

[34] E. A. Plis, D. Engelhart, V. Murray, D. B. A.N. Sokolovskiy, D. Ferguson and R. Hoffman, "Effect of Simulated GEO Environment on the Properties of Solar Panel Coverglasses," *IEEE Transactions on Plasma Science,* vol. 49, no. 5, pp. 1679-1685, 2021.

[35] D. P. Engelhart, V. J. Murray, E. A. Plis, K. Fulford, D. C. Ferguson and R. Hoffmann, "Effect of Electron Flux on the Degradation of Organic Polymers in a Simulated GEO Environment," in *AIAA Scitech 2021 Forum 0066* , 2021.

[36] J. A. Reyes, K. W. Fulford, E. A. Plis, R. C. Hoffmann, V. J. Murray, H. M. Cowardin, D. Cone, D. C. Ferguson, M. T. Bengtson, J. R. Shah and D. P. Engelhart, "Spectroscopic behavior of various materials in a GEO simulated environment," *Acta Astronautica,* vol. 189, pp. 576-583, 2021.

[37] R. Cooper and R. Hoffman, "Jumbo Space Environment Simulation and Spacecraft Charging Chamber Characterization," Air Force Research Laboratory, Space Vehicles Directorate Kirtland AFB United States, Albuquerque, NM, 2015.

[38] M. Bengtson, J. Maxwell, R. Hoffmann, R. Cooper, S. Schieffer, D. Ferguson, W. R. Johnston, H. Cowardin, E. Plis and D. Engelhart, "Optical Characterization of Commonly Used Thermal Control Paints in a Simulated GEO Environment," in *Advanced Maui Optical and Space Surveillance Technologies Conference*, Maui, HI, 2018.

[39] E. M. Albrecht, A. M. Jensen, E. G. Jensen, K. A. Wilson, M. K. Plummer, J. A. Key, D. S. O'Keefe, F. K. Chun, D. M. Strong and C. P. Schuetz-Christy, "Near-Simultaneous Observations of a Geosynchronous Satellite Using Two Telescopes and Multiple Optical Filters," *The Journal of the Astronautical Sciences,* vol. 69, pp. 120-138, 2022.

[40] L. Bradley, B. Sipőcz, T. Robitaille, E. Tollerud, Z. Vinícius, C. Deil, K. Barbary, T. Wilson, I. Busko, A. Donath, H. M. Günther, M. Cara, P. L. Lim, S. Meßlinger, S. Conseil, A. Bostroem, M. Droettboom, E. M. Bray, L. A. Bratholm and e. al., "astropy/photutils: 1.0.0," Zenodo, 13 September 2020. [Online]. Available: https://doi.org/10.5281/zenodo.4044744. [Accessed 22 August 2022].